Journal of Materials Chemistry C

Accepted Manuscript

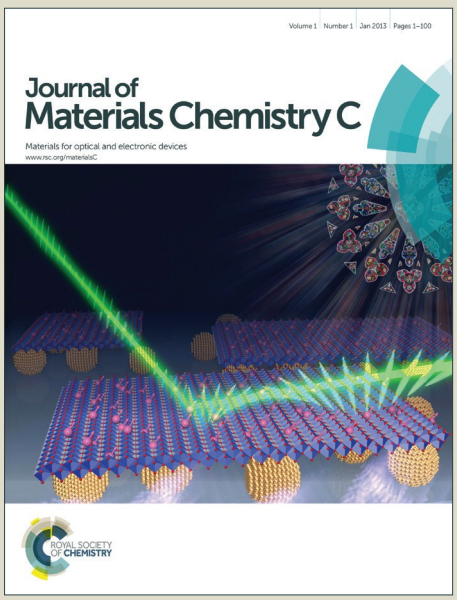

ROYAL SOCIETY OF CHEMISTRY

www.rsc.org/materialsC

$Sr_3Ce(PO_4)_3:Eu^{2+}$: A Broadband Yellow-Emitting Phosphor for Near Ultraviolet-Pumped White Light-Emitting Devices

Pengpeng Dai[1,‡], Szu-Ping Lee[1], Ting-Shan Chan[2], Chien-Hao Huang[3], Yun-Wei Chiang[4], Teng-Ming Chen[1*]

[1]*Phosphors Research Laboratory, Department of Applied Chemistry and Institute of Molecular Science, National Chiao Tung University, Hsinchu 30010, Taiwan*

[2]*National Synchrotron Radiation Research Center, Hsinchu Science Park, Hsinchu 30076, Taiwan.*

[3]*Materials and Chemical Research Laboratories, Industrial Technology Research Institute, Hsinchu 30011, Taiwan*

[4]*Advanced-ESR Lab for Nano-biophysics, Department of Chemistry, National Tsing Hua University, Hsinchu, 30013, Taiwan*

[*] Corresponding author: tmchen@mail.com.edu.tw.

‡ On leave from Center for Advanced Optoelectronic Functional Materials Research, and Key Laboratory for UV-Emitting Materials and Technology of Ministry of Education, Northeast Normal University, 5268 Renmin Street, Changchun 130024, China

Abstract

We have synthesized and investigated a series of yellow-emitting $Sr_3Ce(PO_4)_3:Eu^{2+}$ phosphors, showing extremely broadband at around 535 nm (with FWHM of ca. 200 nm/6,760 cm^{-1}) and large Stoke shift (ca. 8,265 cm^{-1}), which is attributed to the 4f-5d transition of Eu^{2+} without the contribution from Ce^{3+} emission under excitation at long wavelength (> 370 nm). However, such broadband Eu^{2+} emission is rather surprising, considering that there is only one cation site for Eu^{2+} luminescence center. Herein, we investigate the crystal structure by performing X-ray Rietveld refinement on the synchrotron X-ray diffraction data, and demonstrate that both cation and anion sites in $Sr_3Ce(PO_4)_3$ are disordered in the host lattice. These unusual structure characters generate a variety of distinct Eu^{2+} sites, which is verified by the decay lifetime analysis and electron paramagnetic resonance spectra, and thus result in astonishing broadband yellow-emission. Moreover, a white LED device with color-rendering index of 86.5, color temperature of 5,996 K, and chromaticity coordinates of (0.32, 0.38), was obtained by combining a 405 nm near-UV LED chip and the phosphor blends of yellow-emitting $Sr_3Ce(PO_4)_3:Eu^{2+}$ and the commercial blue-emitting $BaMgA_{10}O_{17}:Eu^{2+}$ phosphor. These results indicate that the as-prepared yellow-emitting $Sr_3Ce(PO_4)_3:Eu^{2+}$ phosphor has potential applications in the dual-color-phosphor-converted WLEDs.

Keywords: Yellow-emitting phosphor, $Sr_3Ce(PO_4)_3:Eu^{2+}$, Broadband emission, White light-emitting diodes

1. Introduction

The use of phosphor-converted white light-emitting diodes (pc-WLEDs) continuously drives the advance in the field of inorganic luminescent materials. The major WLEDs presently in the market are fabricated by integrating blue LED and yellow-emitting phosphor (YAG:Ce^{3+}), which is considered to be one of the easiest and the most efficient way for white-light generation.[1,2] However, this type of white-light suffers from poor color rendition ($Ra \leq 80$) because of the weak luminescence in the red spectral region.[3,4] As an improvement, white-light with multi-emission bands is proposed by the combination of the tricolor phosphors with near ultraviolet LED (n-UVLED) chips.[5-7] Unfortunately, such WLEDs devices can be problematic since this method of packaging often induces some problems including energy loss due to reabsorption and color balance.[5-9] To circumvent these drawbacks, one suggestion that has been put forth in this regard is to lower energy loss due to reabsorption by using binary complementary color phosphors for n-UVLED chips, since dual-color phosphors can lower reabsorption energy loss to some extents and meanwhile simplify the fabrication processes of WLEDs.[9,10] In this way, it is required that the yellow-emitting phosphor not only shows a broadband emission with enriched red component but also itself cannot be excited by the blue light.[10] Therefore, the effort to develop suitable yellow-emitting phosphors has been very active.

Recently, a great number of eulytite-type $M^{II}_3Ln^{III}(PO_4)_3$ compounds (where M^{II} = divalent cation, Ln^{III} = trivalent cation) acting as host materials for phosphors have drawn increasing attention due to their chemical and mechanical stability.[11-15] Additionally, eulytite-type

$B^{II}_3M^{III}(PO_4)_3$ compounds can incorporate various foreign ions and provide abundant crystal field environments, which makes it possible to finely tune the physical/chemical properties to design new luminescence materials.[16-18] Recently, several investigations have been reported on Eu^{2+}-doped $B_3M(PO_4)_3$ compounds (B = Ca, Sr, Ba, M = Bi, Gd, Lu and Y) to exhibit novel luminescence properties.[16-18] $Sr_3Ce(PO_4)_3$, crystallized in the eulytite-type structure, has only one cation site 16c (C3 symmetry) in the unit cell, and thus one emission band can generally be expected when Eu^{2+} is doped into host lattice. Herein, we report a yellow-emitting $Sr_3Ce(PO_4)_3:Eu^{2+}$ phosphor, which shows extremely broadband emission at around 538 nm and large Stokes shift. The detailed crystal structure analysis has been investigated by the Rietveld refinement of Synchrotron X-ray diffraction profile, electron paramagnetic resonance (EPR) spectra, and the lifetime decay analysis. We have found that both cation/anion sites are distorted in the host lattice and the extremely broad yellow-emission is confirmed to be originated from a large amount of distinct Eu^{2+} ions induced by the disordered cation/anion sites. Moreover, a WLED with a color-rendering index (Ra) of 86.5, correlated color temperature (CCT) of 5,996 K, and CIE chromaticity coordinates of (0.32,0.38), has been fabricated by using the yellow-emitting $Sr_3Ce(PO_4)_3:Eu^{2+}$ (SCPO:xEu^{2+}), commercial blue-emitting $BaMgAl_{10}O_{17}:Eu^{2+}$ (BAM:Eu^{2+}) and a 405 nm near-UV LED chip. These results indicate that this broadband yellow-emitting SCPO:0.07Eu^{2+} phosphor has a great potential to serve as a phosphor for near-UV pumped WLEDs.

2. MATERIALS AND METHODS

Materials synthesis

Polycrystalline SCPO:xEu^{2+} was synthesized via solid-state reactions using $SrCO_3$ (99.95%), CeO_2 (99.99%), $(NH_4)_2HPO_4$ (99.95%), and Eu_2O_3 (99.99%) as starting materials. Briefly, the powder mixtures in stoichiometric composition were thoroughly mixed using an agate mortar and pestle and subsequently sintered for 4 h at 1450 °C in the air. The obtained samples were reground and fired again for 5 h at 1350 °C in a muffle furnace under reducing atmosphere (10% H_2/90% N_2). Finally, samples were then ground well for further characterization.

Characterization methods

The phase purity of all samples was verified by using powder X-ray diffraction (XRD) with Cu K_α radiation by using a Bruker AXS D8 diffractometer operated at 40 kV and 20 mA. Synchrotron X-ray diffraction (SXRD) pattern of $Sr_3Ce(PO_4)_3$:0.07Eu^{2+} sample was collected at the BL01C2 beamline with energy range within 12-33 keV in the National Synchrotron Radiation Research Center (NSRRC), Taiwan. The structure refinement was carried out using the General Structure Analysis System (GSAS) program.[19] The diffuse reflection spectra were measured with a double-beam UV-vis spectrometer (Hitachi 3010, Japan) equipped with a ∅60 mm integrating sphere. The photoluminescence (PL) and PL excitation (PLE) spectra were measured by using a Horiba FL-3 fluorescence spectrophotometer equipped with a 450 W Xe lamp. The quantum efficiency (QE) was

measured by using a Horiba F-3018 integrating sphere whose inner face was coated with spectralon®. Fluorescence decay time was measured on a tunable nanosecond optical-parametri-oscillator/Q-switch pumped YAG:Nd laser system (Ekspla). EPR spectra was recorded by a JES-FA200 (JEOL, Japan) EPR spectrometer. The WLEDs were fabricated using the phosphor blends of the as-prepared yellow-emitting $Sr_3Ce(PO_4)_3$:0.07Eu^{2+} and the commercial blue-emitting BAM:Eu^{2+} phosphor with a near-ultraviolet LED (n-UVLED) chip (~405 nm). The optical properties, including the electroluminescence (EL) spectra, the Ra values, the CCT, and Commission Internationale de l´Eclairage (CIE) chromaticity coordinates of the WLED were recorded by a SphereOptics integrating sphere with LED measurement starter packages (Onset, Inc.).

3. RESULTS AND DISCUSSION

Figure 1a shows the XRD patterns of polycrystalline $Sr_3Ce(PO_4)_3$:xEu^{2+} ($0 \leq x \leq 0.2$) samples, which all maintain the characteristic patterns of the cubic structure (space group *I43d*) and are consistent with the standard XRD profile of $Sr_3La(PO_4)_3$ (PDF card No.29-1298).[20] No detectable XRD peaks corresponding to impurity phases were observed. However, the XRD peak located at 45.4° in 2θ, corresponding to the (510) crystal plane, shifts slightly to the higher angle direction with increasing Eu^{2+} content (Fig. 1b). These observations indicate that Eu^{2+} ions have been successfully incorporated into the crystal lattice, and substitution of smaller Eu^{2+} (r = 1.17 Å, CN = 6) for Sr^{5+} (r = 1.18 Å, CN = 6) induces size shrinkage of the host. Moreover, the full width at half maximum (FWHM) of the XRD peaks was found to broaden gradually with increasing Eu^{2+} content, which may imply possible distortion of host lattice and random distribution of Eu^{2+} ions. To further

examine the crystal structure and occupancy probability of cation in this compound, the Rietveld refinement was performed by using synchrotron powder X-ray diffraction data. The calculated and experimental results as well as their difference in the XRD refinement of the SCPO:0.07Eu^{2+} sample are shown in Fig. 2a. The initial structural model is established by the standard crystallographic data of $Sr_3La(PO_4)_3$ (ICSD#69431), which is isostructural to SCPO compound and belongs to the $M^{II}_3Ln^{III}(PO_4)_3$-family (cubic, space group *I43d*). Refined structural parameters of SCPO:0.07Eu^{2+} are summarized in Table 1. We have found that Sr^{2+}, Ce^{3+}, and Eu^{2+} ions all occupy the single 16*c* (C3 symmetry) sites in the unit cell. In the refinement process, we presume that 93% of 16*c* sites are filled by Sr and Ce, and 7% by Eu atom without any site-mixing and the temperature factors for Sr, Ce and Eu atoms in 16*c* position are constrained to equality. The final reliability factors for the whole patterns are R_{wp} = 8.72% and R_p = 5.14%, respectively. The refined lattice parameters for $Sr_3Ce(PO_4)_3$ are *a* = 10.169(7) Å, V = 1051.791(1) $Å^3$, which show an apparent lattice shrinkage in comparison with that of $Sr_3La(PO_4)_3$.[19] Figure 2b shows the crystal structure of SCPO and the coordination of Sr and P in the host lattice. It is clearly seen from the Fig. 2c and Table 1 that oxygen atoms, denoted as O1, O2 and O3, are distributed in three 48*e* sites and have the same occupancy probability in this compound. The bond lengths for P-On (n = 1,2,3) are different from each other;[19] for example, the bond length for P-O1, P-O2, P-O3 was found to be 1.529, 1.555, and 1.474 Å, respectively, indicating SCPO compound possibly possesses many PO_4 tetrahedra with different orientations. Therefore, one can imagine that SCPO phase shows not only cation disorder but also disorder in the oxygen sublattice.[11,16,20] Unfortunately, it is impossible to distinguish each of the bond lengths of d(Sr-O1), d(Sr-O2),

and d(Sr-O3) since the X-ray refinement simply reveals an average value of d(Sr/Eu-On). Such a structural character may be responsible for the unusual luminescence properties when Eu^{2+} ions were doped and occupy at the Sr sites in SCPO:xEu^2.

Figure 3 shows the diffuse reflectance spectra for SCPO:xEu^{2+} ($0 \leq x \leq 0.1$) samples, where the Kubelka-Munk absorption coefficient is calculated from the measured reflectance (R%) according to equation (1),

$$F(R) = \frac{(1-R)^2}{2R} \quad (1)$$

The calculation is considered to be necessary to minimize the influence of multiple scattering in powder samples, especially in the region near the absorption edge.[21] The SCPO host exhibits a strong absorption at around 320 nm, which is mainly attributed to the 4f-5d transition of Ce^{3+}, and there is no absorption observed in the visible range and, accordingly, it is white in color. However, Eu^{2+} doping causes an immediate change in the optical properties of SCPO. It is clearly seen that the absorption edge shows a red-shift with increasing Eu^{2+} dopant content, which indicates the successful incorporation of Eu^{2+} ions into the host lattice and this observation is in agreement with the XRD results. We have observed that the sample gradually turns yellow with increasing Eu^{2+} dopant content, indicating that the energy levels of Eu^{2+} ions are localized within the electronic structure of the SCPO host, and provide absorption channels for visible light. .

Figure 4 shows the PL and PLE spectra of the host SCPO. Under excitation at 325 nm, the host SCPO shows a asymmetric broadband emission centered at 402 nm, which is attributed to the transitions of Ce^{3+} from the 5*d* excited state to the $^2F_{5/2}$ and $^2F_{7/2}$ ground states.[22] The PL spectrum can be deconvoluted into two Gaussian bands centered at 24,796

cm^{-1} (~402 nm) and 22,891 cm^{-1} (~435 nm), respectively, with an energy difference of 1,905 cm^{-1} , as shown in supporting information in Figure S1 (See ESI†, Fig. S1), which is close to the energy separation between $^2F_{5/2}$ and $^2F_{7/2}$ levels of Ce^{3+}.[22] The corresponding PLE spectra (monitored at λ_{em} = 402 nm) ranging from 250 to 360 nm is attributed to the 5d-4f transition of Ce^{3+}. When doped with Eu^{2+} ion at the level of 0.01 mol%, the PL spectrum shows an extremely broad-band yellow emission from 400 to 800 nm under excitation at 375 nm (Fig. 5a). The FWHM and Stokes shift of the SCPO:0.01Eu^{2+} sample is estimated to be ~200 nm (8,791 cm^{-1}/~0.797 eV) and 8,380 cm^{-1}(~1.07 eV), respectively. However, both the FWHM and the Stokes Shift for this yellow-emitting phosphor are significantly larger than those reported previously for Eu^{2+}-activated phosphors,[23-26] and even larger than that of the commercial yellow-emitting $(Ba,Sr)_2SiO_4:Eu^{2+}$ phosphor (See ESI†, Fig. S2). In order to investigate the energy transfer from Ce^{3+} to Eu^{2+}, the PL and PLE spectra of SCPO, and PLE spectrum of SCPO:0.07Eu^{2+} are presented in Fig. S3 in ESI†, respectively. It is clearly seen that the PL spectrum of SCPO overlaps well with the PLE spectrum of SCPO:0.07Eu^{2+} in the range of 365-450 nm, indicating the energy transfer from Ce^{3+} to Eu^{2+} can occur when the sample is excited with a shorter wavelength (<360 nm). Therefore, we believe that obtained broadband yellow emission (λ_{ex} =375 nm) totally originates from the 5d→4f transition of Eu^{2+} without the contribution from the Ce^{3+} ions.

With increasing Eu^{2+} dopant content, continuous red shift from 528 to 549 nm is observed in PL spectra under excitation at 375 nm (Fig. 5b), which could be rationalized with spectral reabsorption and increasing crystal fields splitting of Eu^{2+}. In the case of reabsorption, the emission with higher energy generally resonates with the lower energy part of excitation

spectra, resulting in the more energetic emission that is partially reabsorbed, thus shifting the emission spectrum to the red region.[24] In the present study, it is clearly seen that the higher-energy emission overlaps with the lower energy part of the PLE spectra (Fig. 6), and the extent of overlap becomes more prominent with increasing the Eu^{2+} content. In the case of increasing crystal fields splitting of Eu^{2+}, the average interatomic distances between Eu^{2+} ions are expected to be reduced with increasing Eu^{2+} content, and thereby the interaction between two activators becomes much stronger, resulting in an increase of crystal field spitting of the 5d energy levels of Eu^{2+}.[27] For the variations of the crystal field strength, one of the phenomenological characteristics is the change in the wavelength and shape of the PLE spectrum. As shown in Fig. 6, with increasing the Eu^{2+} content, different PLE spectra for emission bands with lower energy confirm the increasing crystal field strength acting on Eu^{2+}.[28,29] The crystal-field splitting of Eu^{2+} increases gradually from 20,414 cm^{-1} for SCPO:xEu^{2+} sample with x = 0.01 to 21,120 cm^{-1} for SCPO:xEu^{2+} sample with x = 0.2 (Table 2). In addition, Table 2 also reveals that the Stokes shift decreases with increasing Eu^{2+} dopant content. Therefore, we believe that the observed red-shifting in PL spectra is attributed to the effects of reabsorption, increasing crystal field spitting of Eu^{2+} and reduced Stokes shift. For the SCPO:0.07Eu^{2+} sample, the luminous intensity reaches a maximum value, and then decreases gradually as a result of concentration quenching when x exceeded 0.07. Furthermore, the external quantum yield (QY) of SCPO:0.07Eu^{2+} was determined to be 50.6 % under excitation at 375 nm.

Fig. 6 shows the normalized PLE spectra of the SCPO:xEu^{2+} phosphors ($0 < x \leq 0.2$) by monitoring the lower-energy emission bands. All the PLE spectra show broad excitation

bands, which are attributed to the 4f-5d transitions of Eu^{2+}/Ce^{3+}. With increasing Eu^{2+} dopant content, the onset of the $4f^{6}5d$ band shifts gradually to the longer wavelength side along with profile change, indicating the changes of crystal field strength acting upon the Eu^{2+} ions. Note that the broad PLE spectra, showing strong absorption at the wavelength range of 380 - 410 nm, match well with the wavelength of the n-UV LED chips, yet show a weak absorption in the blue spectral region. These spectral properties make it possible to fabricate a high CRI WLED by using dual-color phosphors and an n-UV LED chip.

According to the work by Dorenbos,[23] extremely broad Eu^{2+} emission (FWHM of ~200 nm/~6300 cm^{-1}) is rather surprising considering that the crystal structure contains a single cationic lattice site (16*c* sites for Sr and Ce) for the luminescent center. By deconvolution of the emission peak for the SCPO:0.07Eu^{2+} sample, it was found that the broadband emission spectrum requires two Gaussian functions centered at ca. 542 nm (~18,102 cm^{-1}) and 650 nm (~ 14,770 cm^{-1}), respectively, for data fitting. (See ESI†, Fig. S3) Therefore, we speculate that the Eu^{2+} ions very likely occupy more than one cation site in this compound. In the case of multiple Eu^{2+} centers, the lifetime decay profiles for each distinct Eu^{2+} center are different since distinct Eu^{2+} ions with different coordination environments possibly have different de-excitation channels.[30] Consequently, it is expected that once the lifetimes corresponding to the different emission wavelength are determined, the existence of multiple Eu^{2+} centers can be confirmed. To validate the hypothesis, we have measured wavelength-dependent luminescence decays under excitation at 355 nm. A set of luminescence decay curves is recorded for selected samples with x = 0.01 and 0.07 by monitoring the emission at 480, 535 and 650 nm, respectively. For SCPO:0.01Eu^{2+} sample , it is clearly seen that the profiles for

the three decay curves are different from one another (Fig. 7a), and exhibit non-single exponential decay behavior. The decay processes are characterized by an average lifetime, τ, which can be calculated using the equation (1) as follows,[28]

$$\tau = \frac{\int_0^\infty I(t)\, t\, dt}{\int_0^\infty I(t)} \quad (1)$$

where I(t) is the luminous intensity at time t. Based on equation (1), the average lifetimes for the three Eu^{2+} emissions are calculated to be 0.87, 1.15 and 1.25 μs, respectively. The variation of lifetime as a function of the emission wavelength suggests that the local structure around Eu^{2+} ions is different. Similar phenomena have also been observed in the SCPO:0.07Eu^{2+} sample (Fig. 7b) and their average lifetimes for the three emissions are calculated to be 0.87, 1.15 and 1.25 μs, respectively. Herein, it is impossible to distinguish different lifetimes induced by small differences in the local structure. Accordingly, we tentatively assume that the broadband yellow emission originates from a large amount of Eu^{2+} ions with different local structures, which may be resulted from the random distribution of Sr and Ce ions in an identical crystallographic site (site symmetry of C_3). It should also be noted that the higher-energy band decays (λ_{em} = 480 nm) much faster than the lower-energy band, and the nonlinearity of decay curves becomes more prominent, which indicates de-excitation processes of electrons in excited states becomes more complex. It is difficult to give an definite reason why the lifetimes for higher-energy emissions are shorter than those of lower-energy ones. Therefore, we speculate that the energy transfer may take place between Eu^{2+} ions, each of which has a distinct coordination environment, and thus the higher-energy emission may be partially quenched by the so-called "site-to-site" energy transfer.[30] In addition, the contribution of energy transfer from Ce^{3+} to Eu^{2+} cannot be ruled

out completely when the samples are excited at 355 nm.

The EPR technique is an efficient way to probe the local structure of Eu^{2+} ions because the EPR of Eu^{2+} ion ($4f^7$, S = 7/2, L = 0) shows long spin-lattice relaxation times so Eu^{2+} EPR spectrum could be clearly identified.[31-33] To further understand the local environment of Eu^{2+}, the EPR spectra of the selected SCPO:xEu^{2+} powders (x = 0.01 and 0.07) are shown in Fig. 8, respectively. As for the SCPO sample, some weak EPR signals can be detected by enlarging the EPR spectrum (the inset of Fig. 8), which may be attributed to the EPR signals of Ce^{3+} or some kinds of paramagnetic defects in the host. However, the weak EPR signals can be nearly neglected in comparing with that of Eu^{2+} ions. Therefore, we believe that these EPR signals of SCPO:xEu^{2+} (x= 0.01 and 0.07) are attributed to unpaired electrons of Eu^{2+}. Generally, the EPR signals of Eu^{2+} in the lower symmetry site can present fine structure consisting of seven sharp lines resulting from the splitting of J = 7/2 state into 2j+1 levels.[33] The separations between these lines depend on the symmetry around Eu^{2+} ion in the host. For cubic symmetry, all these lines coincide and only a single line will be found.[33] However, the hyperfine structure of Eu^{2+} cannot be observed in the present study. For SCPO:0.01Eu^{2+} sample, the EPR spectrum of Eu^{2+} displays very larger linewidth than that of earlier reported Eu^{2+}-doped phosphors.[31-35] With increasing Eu^{2+} content, it is found that the linewidth of EPR spectra of the selected SCPO:xEu^{2+} (x = 0.01 and 0.09) samples are broadened (Fig. 8), which presents a solid evidence that the interaction between Eu^{2+} and host lattice becomes more prominent with increasing Eu^{2+} dopant content, leading to an increase of 5d energy level splitting of Eu^{2+}, thus causing a red-shift of PL spectra,[36] which is agreement with the results of PL/PLE spectra. Interestingly, we also found that the obtained Eu^{2+} EPR

spectra are similar to those of Eu^{2+}-doped glass/ceramics, such as the glass with composition of $33NaPO_3$-$66Sr(PO_3)_2$:Eu^{2+} (NSP),[37] another glass with composition of $Sr(PO_3)_2$-$10MgF_2$-$30CaF_2$-$15SrF_2$-$35AlF_3$:Eu^{2+} (FP),[37] and Eu^{2+}-doped fluorozirconate glass ceramics (ZBLAN).[38] It is well-known that the EPR spectrum of Eu^{2+}-doped glass/ceramic is a good example of so-called U-spectrum originated from superimposing by an additional EPR spectrum.[37-39] Brobeck and Iton reported that the U-spectrum is a characteristic of (1) Eu^{2+} sites with a very low symmetry or disordered coordination environment; (2) Eu^{2+} sites with a broad symmetry distribution.[39] Based on our EPR results and previous EPR analysis of Eu^{2+} ions in glass/ceramic, we believe that the broadband yellow-emission originates from a large number of distinct Eu^{2+} sites with a low symmetry.

Fig. 9 shows the CIE chromaticity diagram of SCPO:xEu^{2+} ($0.01 \leq x \leq 0.2$) under excitation at 365 nm. With increasing Eu^{2+}-dopant content, it is clearly seen that the color tone shifts gradually from yellowish-green to yellow, indicating this phosphor can be serve as a yellow-emitting component for WLED application. The CIE coordinates of SCPO:xEu^{2+} ($0.01 \leq x \leq 0.2$) sample are determined to be (0.348, 0.441), (0.351, 0.443), (0.358, 0.446), (0.368, 0.463), (0.356, 0.437), (0.378, 0.459), and (0.391, 0.470), respectively. Moreover, their CCT values are estimated to be 5143, 5071, 4904, 4721, 4929, 4488, and 4263 K, respectively. The corresponding images (λ_{ex} = 365 nm) are displayed in the inset of Fig. 9 and $Sr_3Ce(PO_4)_3$:Eu^{2+} exhibits a bright yellow emission under excitation at 365 nm. Thus, it is highly feasible to fabricate a high-CRI WLED by using the two-color phosphors. To evaluate the potential application of $Sr_3Ce(PO_4)_3$:$0.07Eu^{2+}$ in the WLED, the WLED is fabricated by using the phosphor blends of as-prepared yellow phosphor and the commercial

blue-emitting BAM:Eu^{2+} with a 405 nm NUV chip. Figure 10 shows the EL spectrum of the fabricated WLED driven at 350 mA. As expected, a full-color white-lighting can be realized. It is clearly seen that the near ultraviolet emission band at around 400 nm, blue-emission band corresponding to the BAM:Eu^{2+} phosphor at around 454 nm, and the yellow-emission band corresponding to the SCPO:0.07Eu^{2+} phosphor at around 540 nm. The as-prepared WLED shows a good Ra of 86.5, the CCT of ~ 5,996 K, and the color chromaticity coordinate of (0.32, 0.38). However, the thermal quenching temperature of BAM:Eu^{2+} phosphor is around 550 ^{o}C, which is much higher than that (~ 80^{o}C) of as-prepared yellow-emitting SCPO:Eu^{2+} phosphor.[40,41] The low thermal quenching temperature for SCPO:Eu^{2+} yellow-emitting phosphor might be attributed to Eu^{2+} ions with the weak structure environment induced by the distorted cation/anion sites. Different thermal quenching temperature for the two phosphors may induce some problems including color balance and chemical stability of WLEDs. In this research our results show that $Sr_3Ce(PO_4)_3$:Eu^{2+} could be a promising yellow phosphor for dual-color- pc-WLED.

4. Conclusion

A series of $Sr_3Ce(PO_4)_3$:Eu^{2+} phosphors with eulytite structure were synthesized by solid-state reactions. Extremely broad-band emission centered at 538 nm and large Stokes shift are found in these yellow-emitting phosphors under excitation at 375 nm. Based on the crystal structure analysis and XRD Rietveld refinement, it is found that the eulytite-type $Sr_3Ce(PO_4)_3$:Eu^{2+} exhibits an unusual structure character, and both cation and anion are distorted in the crystal lattice, which induces a large amount of Eu^{2+} ions with different local

environments. The decay lifetime and EPR spectra of Eu^{2+} indicate that the broad-band yellow-emission is attributed to the distinct Eu^{2+} ions. Moreover, a WLED, fabricated by integrating a 405-nm UV LED chip with phosphor blends of yellow-emitting $Sr_3Ce(PO_4)_3$:$0.07Eu^{2+}$ and the blue-emitting $BaMgAl_{10}O_{17}$:Eu^{2+}, exhibits bright white-light with a CCT of 5,996 K, Ra of 86.5, and CIE of (0.32,0.38). These results indicate that the yellow-emitting phosphors show a great potential for near-UV WLED application.

Acknowledgements

We acknowledge the financial support from Ministry of Science and Technology of Taiwan under Contract Nos MOST 104-2113-M-009-018-MY3 and MOST 103-2811-M-009 -081.

References:

1 H.Yamamoto, *Proc SPIE.,* 2010, **7598,** 759808-759811

2 N. C. George, K. A. Denault and R. Seshadri, *Annu. Rev. Mater. Res.,* 2013, **43,** 2.

3 X. F. Li, J. D. Budai, Liu, F, J. Y. Howe, J. H. Zhang, X. J. Wang, J. G. Zhan, C. J. Sun, R. S. Meltzer and Z. W. Pan, *Light: Science & application.,* 2013, **2**, e50.

4 M. M. Shang, C. X. Li and J. Lin, *Chem. Soc. Rev.,* 2014, **43,** 1372-1386.

5 J. Mckittrick, M. E. Hannah, A. Piquette, J. K. Han, J. I. Choi, M. Anc, M. Galvez, H. Lugauer, J. B. Talbot and K. C. Mishra, *ECS J. Solid State Sci. Technol.,* 2013*,* **2,** R213-R217.

6 H. A. Hoppe, *Angew. Chem. Int. Ed.,* 2009, **48,** 3572-3582.

7 T. Taguchi, *Proc. of SPIE.,* 2009, **7422,** 7420B-1

8 X. Chen, P. P. Dai, X. T. Zhang, C. Li, S. Lu, X. L. Wang, Y. Jia and Y. C. Liu, *Inorg. Chem.,*

2014, **53,** 3441-3448.

9 T. Taguchi, *IEEJ Trans.*, 2008, **3,** 21–26.

10 H. Daicho, T. Iwasaki, K. Enomoto, Y. Sasaki, Y. Maeno, Y. Shinomiya, S. Aoyagi, E. Nishibori, M. Sakata, H. Sawa, S.Matsuishi and H. Hosono, *Nat. Commun.,* 2012, **3,** 1132.

11 N. Guo, Y. H. Zheng, Y. C. Jia. H. Qiao and H. P. You, *New J. Chem.,* 2012, **36,** 168.

12 N. Guo, Y. J. Huang, M. Yang, Y. H. Song, Y. H. Zheng and H. P. You, *Phys. Chem. Phys. Chem*., 2011, **13,** 15077.

13 N. Guo, W. Lu, Y. C. Jia, W. Z. Lv, Q. Zhao and H. P. You, *Chemphyschem*., 2013, **14,** 192.

14 N. Guo, X. Y. Zhang, Y. C. Jia, H. Qiao and H. P.You, *J. Phys. Chem. C.,* 2012, **116,** 1329.

15 N. Guo, Y. J. Huang, Y. C. Jia, W. Z. Lv, Q. Zhao, W. Lu, Z. G. Xia and H. P. You, *Dalton Trans.,* **2013,** 42, 941.

16 Z. Y. Wang, Z. G. Xia, M. S. Molokeev, V. V. Atuchin and Q. L. Liu, *Dalton Trans.,* **2014,** 43, 16800-16804.

17 H. B. Liang, Y. Tao, J. H. Xu, H. He, H. Wu, W. X. Chen, S. P. Wang and Q. Su, *J Solid. State. Chem.,* 2004, **177,** 901-908.

18 A. C. Larson and D. R. Von, *Los. Almos. Natl. Lab. Rep.* 2000, 86-748.

19 JCPDF Card. No. 29-1298.

20 J. Barbier, *J. Solid. State. Chem.,* 1992, **101,** 249.

21 P. P. Dai, X. T. Zhang, X. H. Li, G. R.Wang, C. J. Zhao and Y. C. Liu, *J. Lumin.,* 2011, **131,** 653-656.

22 A. Kalaji, M. Mikami and A. K. Cheetham, *Chem. Mater.,* 2014, **26,** 3966-3975.

23 P. Dorenbos, *J. Lumin.,* 2003, **104,** 239-260.

24 F. Liu, R. S. Meltzer, X. F. Li, J. D. Budai, Y-S. Chen and Z. W. Pan, *Sci. Rep.,* 2014, **4,** 7101.

25 W. J. Ding, J. Wang, Z. M. Liu, M. Zhang, Q. Su and J. K. Tang, *J. Electrochem. Soc.,* 2008, **155,** J122-J127.

26 T-G. Kim, T. Kim, J. Kim, S-J. Kim and S-J. Im, *J. Phys. Chem. C.,* 2014, **118,** 12428-12435.

27 V. Bachmann, C. Ronda, O. Oeckler, W. Schnick and A. Meijerink, *Chem. Mater.,* 2009, 316-325.

28 P. P. Dai, X. T. Zhang, L. L. Bian, S. Lu, Y. C. Liu and X. J. Wang, *J. Mater. Chem. C.,* 2013, **1,** 4570-4576.

29 R. J. Xie, N. Hirosaki, T. Suehiro, F. F. Xu and M. Mitomo, *Chem. Mater.,* 2006, 5578-5583.

30 S. J. Lee and K-S. Sohn, *Opt. Letts.,* 2010, **35,** 1004-1006.

31 V Singh, R. P. S. Chakradhar, J. L. Rao, I. Ko and H-Y. Kwak, *J. Lumin.,* 2010, **130,** 703-708.

32 V. R. Kumar, K. V. Narasimuhulu, N. O. Gopal, J. L. Rao and R. P. S. Chakradhar, *Phys. B.,* 2004, **348,** 446-453.

33 V. Singh, J-J. Zhu, M. Tiwar, M. Soni, M. Aynayas, S-H. Hyun, R. Narayanan, M. Mohapatra and V. Natarajan, *J. Non.-Cry. Solids.,* 2009, **355,** 2491-2495.

34 T. Nakamura, T. Takeyama, N. Takahashi, R. Jagannathan, A. Karthikeyani, G. M. Smith and P. C. Riedi, *J. Lumin.,* 2003, **102,** 369-372.

35 V. Natarajan, M. K. Bhide, A. R. Dhobale, S. V. Godbole, T. K. Seshagiri, A. G. Page and C-H. Lu, *Mater. Res. Bull*., 2004, **39,** 2065-2075.

36 Y. Z. Xu, *Applied Electron Magnetic Resonance Spectroscopy*. China Science Press, Beijing, 2008.

37 H. Heidepriem-Ebendorff and D. Ehrt, *J. Phys.:Condens. Matter.,* 1999, **11,** 7627-7634.

38 S. Schweizer, G. Corradi, A. Edgar and J-M. Spaeth, *J. Phys: Condens. Matter.,* 2001, **13,** 2331-2338.

39 E. Maichukova and B. Boizot, *Mater. Res. Bull.,* 2010, **45(9)**, 1299-1303.

40 S. M. Manh and T. P. N. Thuy, *Intern. J. Eng. Innov. Tech.,* 2013, **3(6),** 67-70.

41 G. Bizarri and B.Moine, *J. Lumin.,* 2005, **113,** 199-213.

Figure captions:

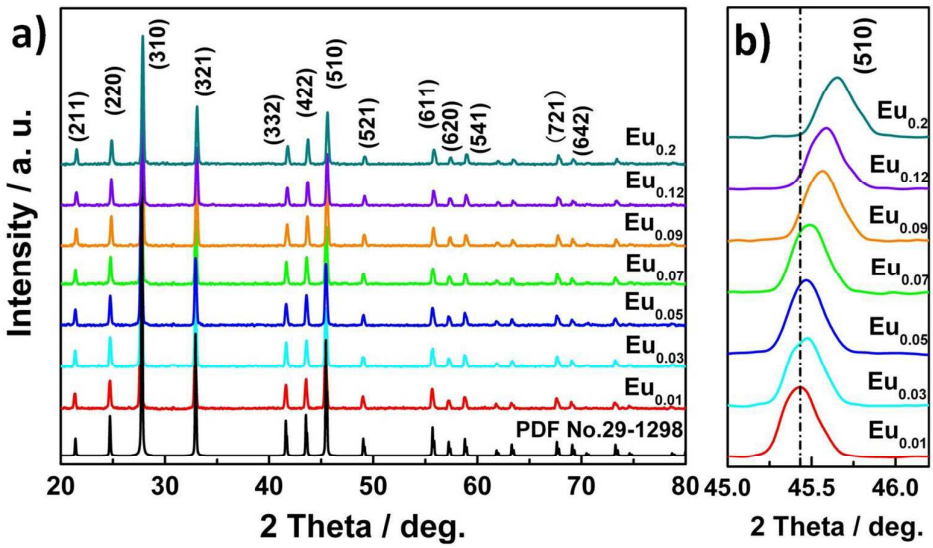

Fig. 1 a) XRD patterns of the SCPO:xEu^{2+} phosphor as a function of Eu^{2+} content. As a reference, the standard XRD data for $Sr_3La(PO_4)_3$ (PDF Card. No 29-1298) is shown. b) Magnified XRD patterns in the region 45 and 46 degrees for the SCPO:xEu^{2+} phosphors as a function of Eu^{2+} content.

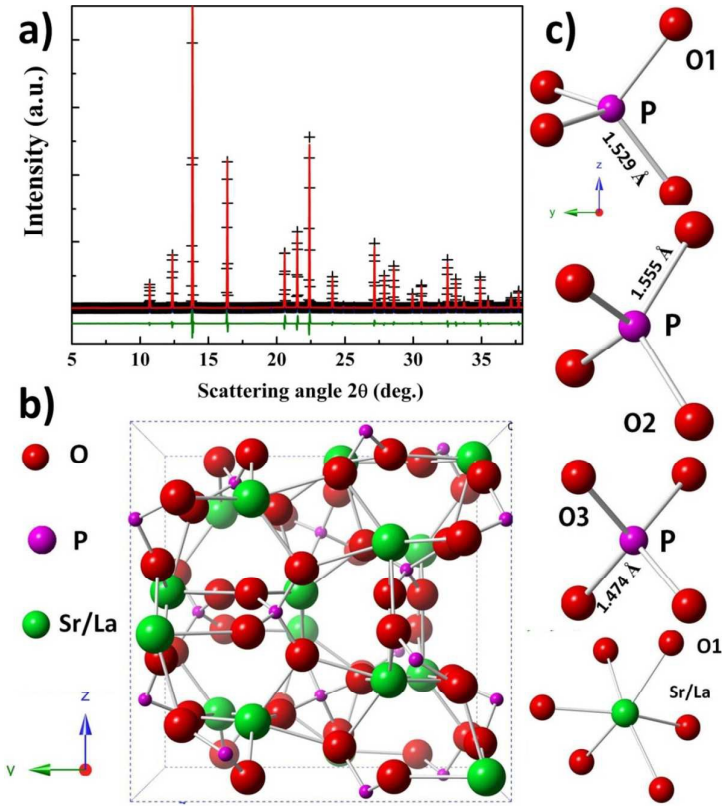

Fig. 2 a) Experimental (cross), calculated (solid line) and difference (bottom) synchrotron power X-ray diffraction patterns for the sample SCPO:0.07Eu^{2+} by the Rietveld refinement method. b) Crystal structure of the sample SCPO and c) the coordination of Sr/P with different oxygen atoms.

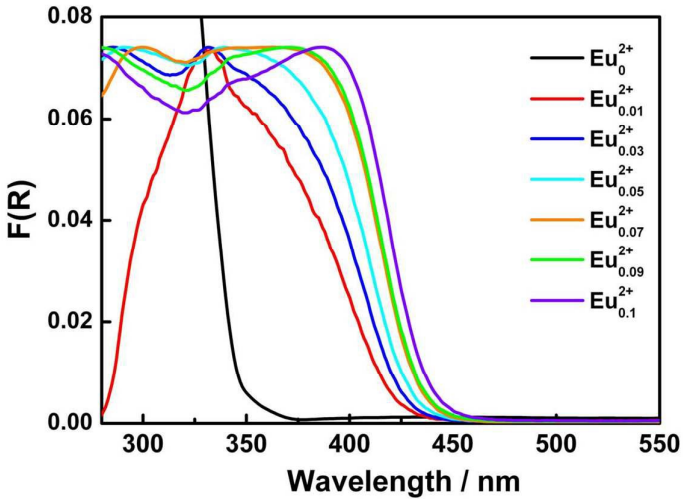

Fig. 3 UV-vis absorption spectra of SCPO:xEu^{2+} powders ($0 \leq x \leq 0.1$) converted from diffuse reflection spectra by the Kubelka-Munk function.

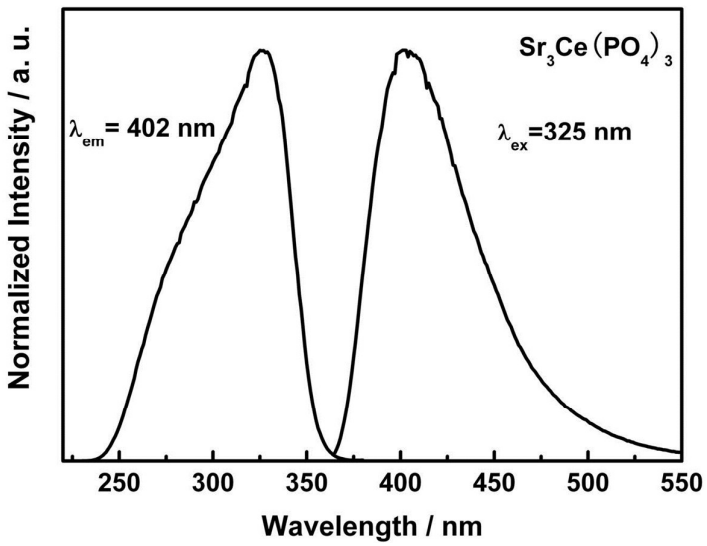

Fig. 4 The normalized PL (λ_{ex} =325 nm) and PLE (λ_{em} =402 nm) spectrum of the host SCPO.

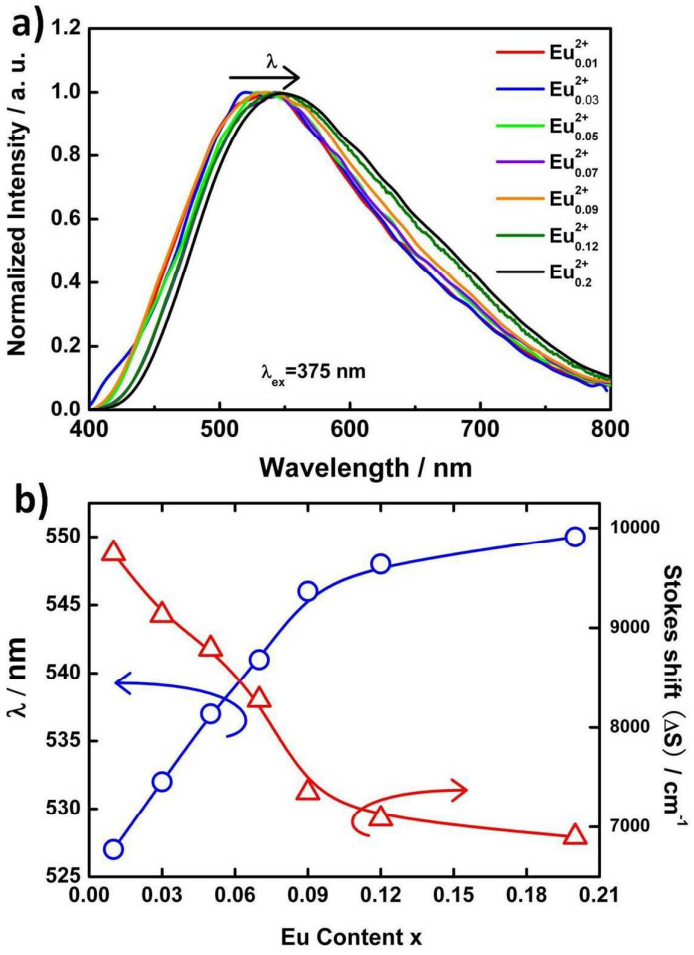

Fig. 5 a) The PL spectra of the SCPO:xEu^{2+} phosphors ($0.01 \le x \le 0.2$) under excitation at 375 nm. b) The dependence of the Stokes shift (ΔS) and the λ_{em} on Eu^{2+} content.

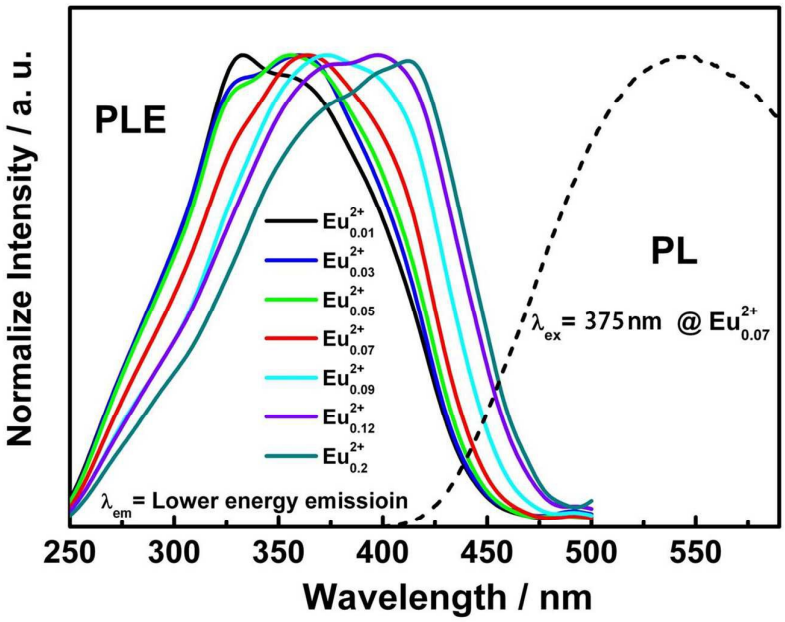

Fig. 6 The normalized PLE spectra of the SCPO:xEu^{2+} phosphors ($0.01 \leq x \leq 0.2$) by monitoring the lower energy emission. Besides, the PL spectrum of SCPO:0.07Eu^{2+} under excitation at 365 nm is also shown in Fig. 6 as a reference.

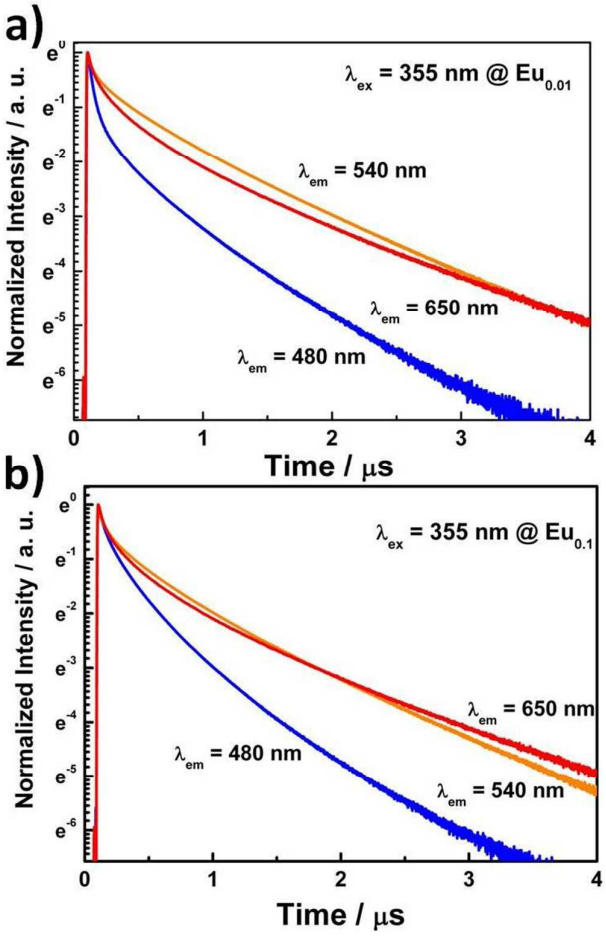

Fig. 7 The lifetime decay curves of the SCPO:xEu^{2+} phosphors with x = (a) 0.01 and (b) 0.1 under excitation at 375 nm by monitoring the emission at 480, 540 and 650 nm, respectively.

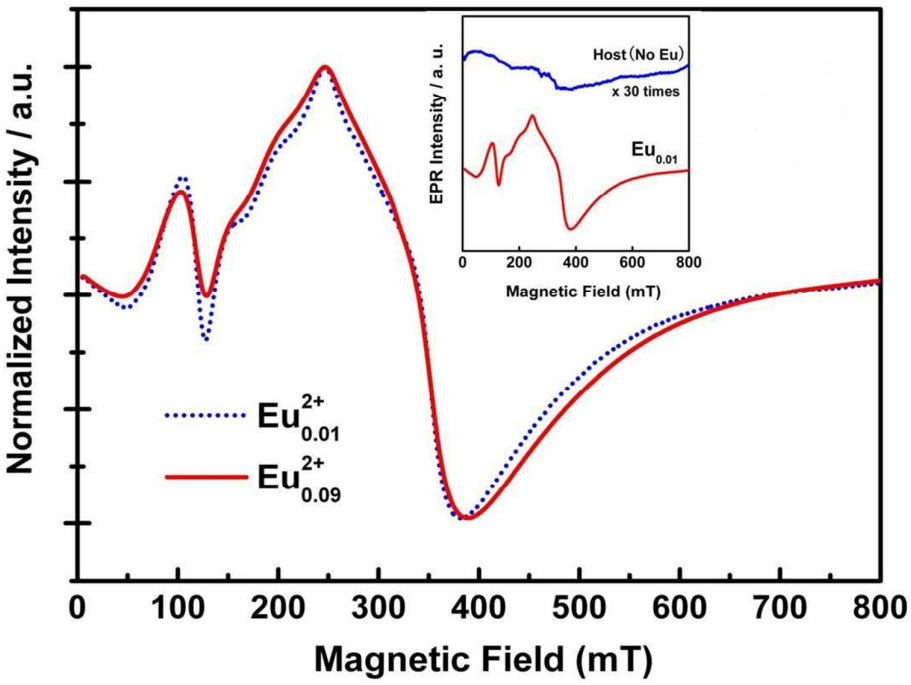

Fig. 8 The EPR spectra of the selected samples SCPO:xEu^{2+} (x = 0.01 and 0.09). The inset presents the EPR spectra of the host SCPO and SCPO:0.01Eu^{2+} as references.

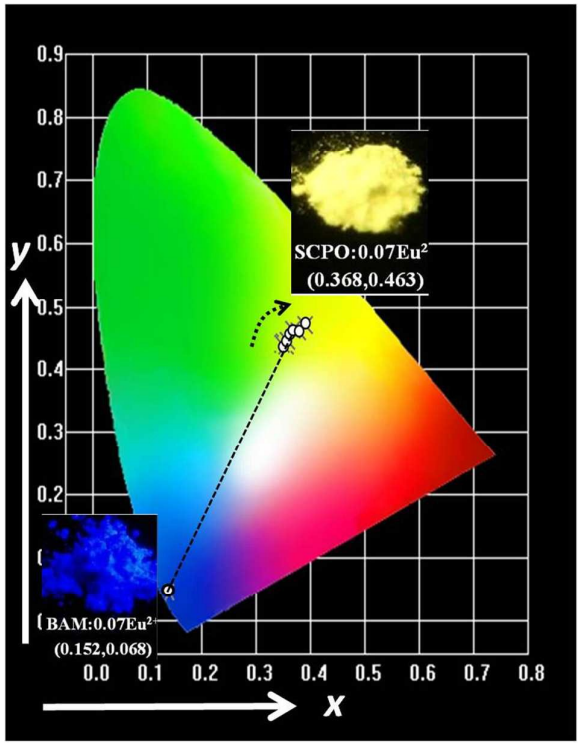

Fig. 9 The CIE chromaticity coordinates of the SCPO:xEu^{2+} (x = 0.01, 0.03, 0.05, 0.07, 0.09, 0.12, 0.2) and the commercial blue-emitting phosphor (BAM:Eu^{2+}) under excitation at 365 nm. The insets show the digital photos and the corresponding the CIE chromaticity coordinates of yellow-emitting SCPO:0.07Eu^{2+} phosphor and commercial blue-emitting phosphor.

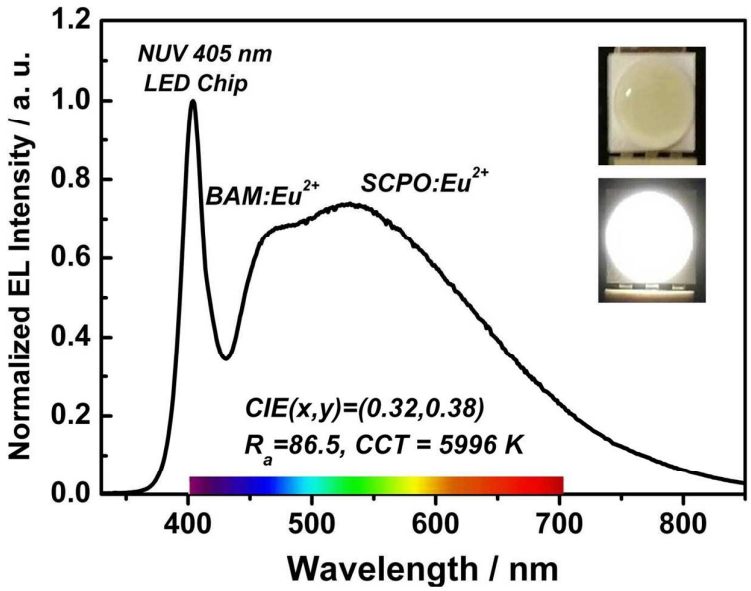

Fig. 10 The EL spectrum of WLED fabricated by using a 405 nm NUVLED chip and the phosphor blends of blue-emitting phosphor (BAM:Eu^{2+}) and the yellow-emitting phosphor (SCPO:Eu^{2+}) under the forward-bias current of 350 mA. The insets show the photographs of as-prepared WLED driven by 350 mA current.

Table Lists:

Table 1 Refined structural parameters for SCPO:0.07Eu^{2+}.

Atom	Wyckoff symbol	X	Y	Z	Occupancy
Sr	16c	0.06245(15)	0.06245(15)	0.06245(15)	0.68
Ce	16c	0.06245(15)	0.06245(15)	0.06245(15)	0.25
Eu	16c	0.06245(15)	0.06245(15)	0.06245(15)	0.07
P	12a	0.375000	0.000000	0.250000	1
O1	48e	0.0439(61)	0.1326(35)	0.2925(47)	0.3333
O2	48e	0.9637(25)	0.1300(28)	0.3023(37)	0.3333
O3	48e	0.0926(33)	0.3304(26)	0.4469(29)	0.3333

Table 2 The PL and PLE bands, Stokes Shift, and crystal field splitting of SCPO:xEu^{2+} (x = 0.01, 0.03, 0.05, 0.07, 0.09, 0.12, 0.2).

Content	λ_{em} (nm)	FWHM of λ_{em} (nm)	λ_{ex} (nm)	Crystal field splitting (cm^{-1})	Stokes shift (cm^{-1})	Normalized PL Intensity (100%)
$Eu_{0.01}$	528	212	346	20,414	11,256	37.5
$Eu_{0.03}$	530	196	350	20,414	8,377	72.5
$Eu_{0.05}$	533	195	351	20,428	8,265	84
$Eu_{0.07}$	535	195	363	20,700	8,295	100
$Eu_{0.09}$	535	207	375	20,888	7,354	76
$Eu_{0.12}$	540	207	398	20,969	7,354	66
$Eu_{0.2}$	544	210	413	21,120	7,354	46

Graphical Abstract

White lighting-emitting diodes (WLEDs) using binary complementary color phosphors for n-UVLED chips are highly expected to realize a lighting source with high color rendering index and high luminous efficiency.